



HAL
open science

Co-crystals of an organic triselenocyanate with ditopic Lewis bases recurrent chalcogen bond interactions motifs

A.M.S. Riel, O. Jeannin, O.B. Berryman, M. Fourmigué

► To cite this version:

A.M.S. Riel, O. Jeannin, O.B. Berryman, M. Fourmigué. Co-crystals of an organic triselenocyanate with ditopic Lewis bases recurrent chalcogen bond interactions motifs. *Acta Crystallographica Section B: Structural Science, Crystal Engineering and Materials* [2014-..], 2019, 75 (1), pp.34-38. 10.1107/S2052520618017778 . hal-02051164

HAL Id: hal-02051164

<https://univ-rennes.hal.science/hal-02051164>

Submitted on 10 Oct 2022

HAL is a multi-disciplinary open access archive for the deposit and dissemination of scientific research documents, whether they are published or not. The documents may come from teaching and research institutions in France or abroad, or from public or private research centers.

L'archive ouverte pluridisciplinaire **HAL**, est destinée au dépôt et à la diffusion de documents scientifiques de niveau recherche, publiés ou non, émanant des établissements d'enseignement et de recherche français ou étrangers, des laboratoires publics ou privés.

Co-crystals of an organic tris-selenocyanate with ditopic Lewis bases: recurrent chalcogen bond (ChB) interactions motifs

Asia Marie S. Riel,^{a,b} Olivier Jeannin,^a Orion B. Berryman,^b and Marc Fourmigué^{*,a}

^a Univ Rennes, CNRS, ISCR (Institut de Sciences Chimiques de Rennes), UMR 6226, 35000 Rennes, France

^b Department of Chemistry and Biochemistry, University of Montana, 32 Campus Dr., Missoula MT 59812, USA

Abstract

Organic selenocyanates R–Se–CN can act as amphoteric chalcogen bond (ChB) donor (through the Se atom) and ChB acceptor (through the nitrogen lone pair). Co-crystallization of the trisubstituted 1,3,5-tris(selenocyanatomethyl)-2,4,6-trimethylbenzene (**1**) is investigated with different ditopic Lewis bases acting as chalcogen bond (ChB) acceptors to investigate the outcome of the competition, as ChB acceptor, between the nitrogen lone pair of the SeCN group and other Lewis bases involving pyridinyl or carbonyl functions. In the presence of tetramethylpyrazine (TMP), benzoquinone (BQ) and *para*-dinitrobenzene (*p*DNB) as ditopic Lewis bases, a recurrent oligomeric motif stabilized by six ChB interactions is observed, involving six SeCN groups and the ChB acceptor sites of TMP, BQ and *p*DNB in the 2:1 adducts (**1**)₂•TMP, (**1**)₂•BQ and (**1**)₂•*p*DNB.

Introduction

Following extensive investigations on halogen bonding interactions as a rediscovered tool in crystal engineering (Cavallo *et al.*, 2016; Gilday *et al.*, 2015) recent approaches have highlighted the generality of the σ -hole concept (Cavallo *et al.*, 2014), and its extension to chalcogen (S, Se, Te), pnictogen (P, As, Sb) and tetrel (Si, Ge, Sn) elements. Halogen atoms are well known to develop one single σ -hole in the prolongation of the C–X bond, allowing for an unprecedented predictability in crystal engineering strategies. The situation is rather different with chalcogens since the presence of two covalent bonds leads to the apparition of two σ -holes (Wang & Zhang, 2009; Alkorta *et al.*, 2018; Bleiholder *et al.*, 2006), as theoretically analyzed in model compounds (Poltizer *et al.*, 2017; Pascoe *et al.*, 2017; Bauzá *et al.*, 2018), and

experimentally illustrated in the crystal structures of $\text{Se}(\text{CN})_2$ (Klapötke *et al.*, 2004; Klapötke *et al.*, 2008), selenophthalic anhydride (Brezgunova *et al.*, 2013) or tellurophene derivatives (Benz *et al.*, 2016; Sánchez-Sanz & Trujillo, 2018). Similar to halogen bonding, chalcogen bond donors are also investigated as Lewis acids in catalysis (Wonner *et al.*, 2017; Benz *et al.*, 2018). We recently postulated that the unsymmetrical substitution of the chalcogen atom, for example in organic selenocyanates $\text{R}-\text{Se}-\text{CN}$ could strongly favor one σ -hole over the other. We found indeed that crystal structures of organic selenocyanates exhibit a recurrent supramolecular motif where the Se atom interacts with the lone pair on the N atom of a neighboring SeCN moiety (Jeannin *et al.*, 2018), leading to the formation of extended chains $\cdots\text{Se}(\text{R})\text{CN}\cdots\text{Se}(\text{R})\text{CN}\cdots$, most probably stabilized by cooperativity. The formation of these motifs is hindered when the selenocyanate is faced with stronger Lewis bases (as 4,4'-bipyridine) and the Se atoms then interact with the pyridinic nitrogen atom, with an even shorter $\text{Se}\cdots\text{N}$ distance (Huynh *et al.*, 2017). Intermolecular (Maartmann-Moe *et al.*, 1984) as well as intramolecular (Wang *et al.*, 2018) $\text{Se}\cdots\text{O}_2\text{N}-$ interactions can also displace the nitrogen atom of the SeCN moiety from interaction with a neighboring Se atom.

In the course of our investigations of the solid-state arrangement of benzylic selenocyanates, we turned our attention to tris-substituted derivatives such as 1,3,5-tris(selenocyanatomethyl)-2,4,6-trimethylbenzene **1**. It was found to crystallize either alone, as a solvate with DMF or AcOEt (Jeannin *et al.*, 2018). In the three structures, we confirmed the formation of recurrent linear ChB motifs where the lone pair of the nitrogen atom in the $\text{R}-\text{Se}-\text{CN}$ moiety interacts as Lewis base with the σ -hole located on the Se atom, essentially in the prolongation of the $\text{NC}-\text{Se}$ bond. As shown in Figure 1a for the DMF solvate, i.e. (**1**)•DMF, this interaction pattern was complemented with a side interaction between the Se atom and the oxygen atom of DMF. On the other hand, in the AcOEt solvate (Figure 1b), the carbonyl oxygen atom displaces one nitrogen atom of a SeCN group to enter into a strong $\text{Se}\cdots\text{O}=\text{C}(\text{OEt})\text{Me}$ interaction (Jeannin *et al.*, 2018). A question then arises about the outcome of the ChB competition of a given Se atom as ChB donor, when interacting either with the N atom of a neighboring SeCN moiety or with another Lewis base. We report here on the outcome of the co-crystallization of **1** with three different ditopic Lewis bases, namely tetramethylpyrazine (TMP), benzoquinone (BQ) and *para*-dinitrobenzene (*p*DNB), allowing us to evaluate the robustness of these one-dimensional $\cdots\text{Se}(\text{R})\text{CN}\cdots\text{Se}(\text{R})\text{CN}\cdots$ motifs.

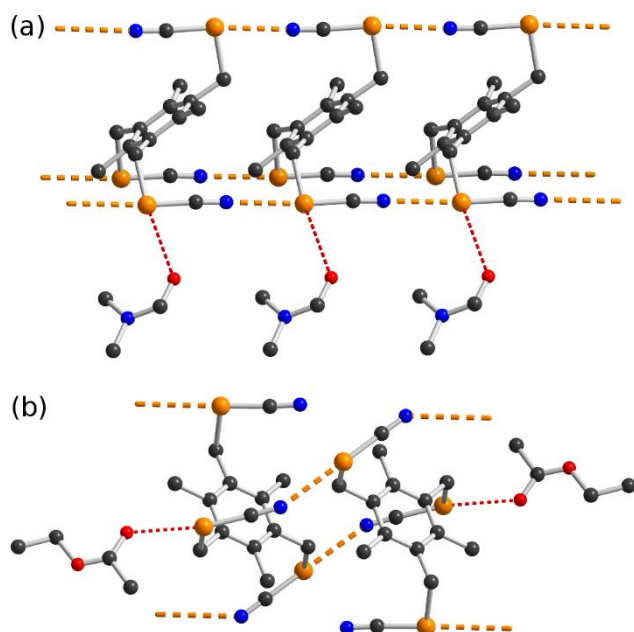


Figure 1. Details of the ChB interactions (orange thick dotted lines for the Se...N interactions, red thin dotted lines for the Se...O interactions) in the solvates of **1** with: (a) DMF, (b) AcOEt. Hydrogen atoms were omitted for clarity. Only one of the two disordered AcOEt molecules in (b) is shown.

Results and Discussion

Co-crystallization of **1** with either TMP, BQ or *p*DNB was performed by mixing solutions of both partners in ethyl acetate and diffusing the mixture with diethyl ether. Crystals formed after two days. All three co-crystals crystallize in the triclinic system, space group $P\bar{1}$, with the tris-(selenocyanate) derivative **1** in the general position in the unit cell, and the ditopic ChB acceptor on the inversion center, hence the 2:1 stoichiometry, that is $(\mathbf{1})_2 \cdot \text{TMP}$, $(\mathbf{1})_2 \cdot \text{BQ}$ and $(\mathbf{1})_2 \cdot p\text{DNB}$. The three structures are closely related (Figure 2). Among the three independent SeCN groups in **1**, two are engaged in a Se...N \equiv C ChB while the third one is engaged in a ChB with the oxygen or nitrogen atom of the coformer, TMP, BQ or *p*DNB. It gives rise locally to the recurring of inversion-centered oligomeric ChB motifs shown in Figure 3.

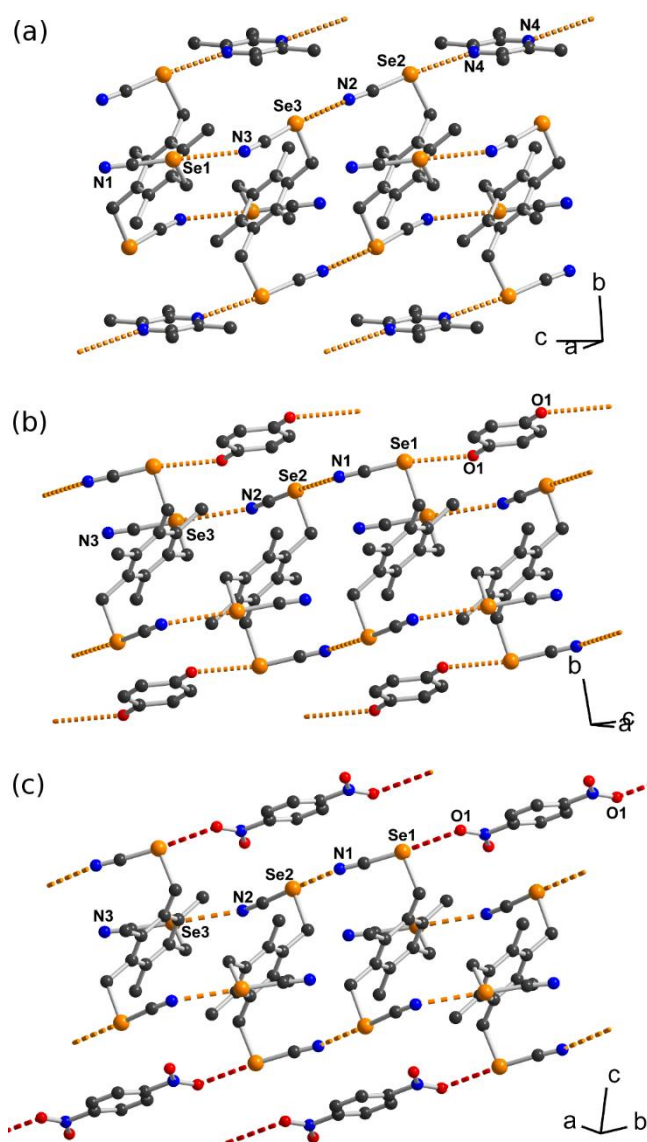


Figure 2. Detail of the ChB interactions in (a): $(1)_2 \bullet \text{TMP}$, (b): $(1)_2 \bullet \text{BQ}$ and (c): $(1)_2 \bullet p\text{DNB}$. Hydrogen atoms have been omitted for clarity. The ChB interactions are indicated as orange ($\text{Se} \cdots \text{N}$) or red ($\text{Se} \cdots \text{O}$) dotted lines.

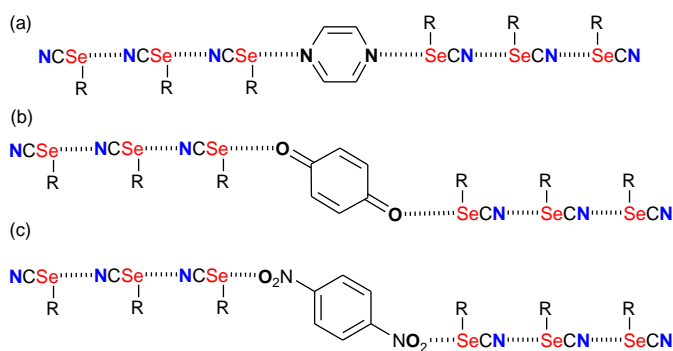
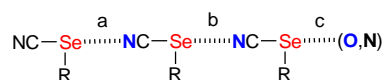


Figure 3. Schematic representation of the oligomeric chalcogen-bonded motifs found in (a): $(1)_2 \bullet \text{TMP}$, (b): $(1)_2 \bullet \text{BQ}$ and (c): $(1)_2 \bullet p\text{DNB}$.

Table 1. ChB characteristics

	ChB a		ChB b		ChB c		Ref
	Se...N (Å)	C-Se...N (°)	Se...N (Å)	C-Se...N (°)	Se...N,O (Å)	C-Se...N,O (°)	
TMP	3.096(6)	178.8(2)	3.029(11)	175.0(2)	3.171(11) (N)	172.6(2) (N)	this work
BQ	3.315(15)	177.1(3)	3.192(10)	174.6(3)	2.966(13) (O)	170.7(3) (O)	this work
<i>p</i> DNB	3.063(20)	178.8(2)	2.989(9)	175.3(2)	3.231(11) (O)	161.9(2) (O)	this work
AcOEt	3.174(4)	177.0(1)	2.965(3)	174.9(1)	2.925(6) ^a (O)	166.5(2) (O)	Jeannin
					2.871(3) ^a (O)	168.8(2) (O)	<i>et al.</i>
							2018

^a The oxygen atom of the carbonyl group in AcOEt is disordered on two equiprobable positions.

The comparison of the ChB characteristics within the three compounds (See Table 1) shows a large dispersion of the Se...N≡C ChB distances, from 2.96 to 3.31 Å, that is a reduction ratio (RR) relative to the sum of the van der Waals radii (1.90 + 1.55 = 3.45 Å) in the range 0.86–0.96. The Se...O ChB contacts are slightly shorter, with RR down to 0.86, in line with the smaller van der Waals radius of O (1.52 Å) vs. N (1.55 Å).

The closely related structural motifs found in (1)₂•TMP, (1)₂•BQ and (1)₂•*p*DNB, are also found in their solid-state organization in the crystal. As shown indeed in Figure 4, we note the recurrent formation of stacks of **1**, interconnected through the Se...N(O, N) ChB interaction with TMP, BQ or *p*DNB molecules acting as ditopic ChB acceptors between the chains.

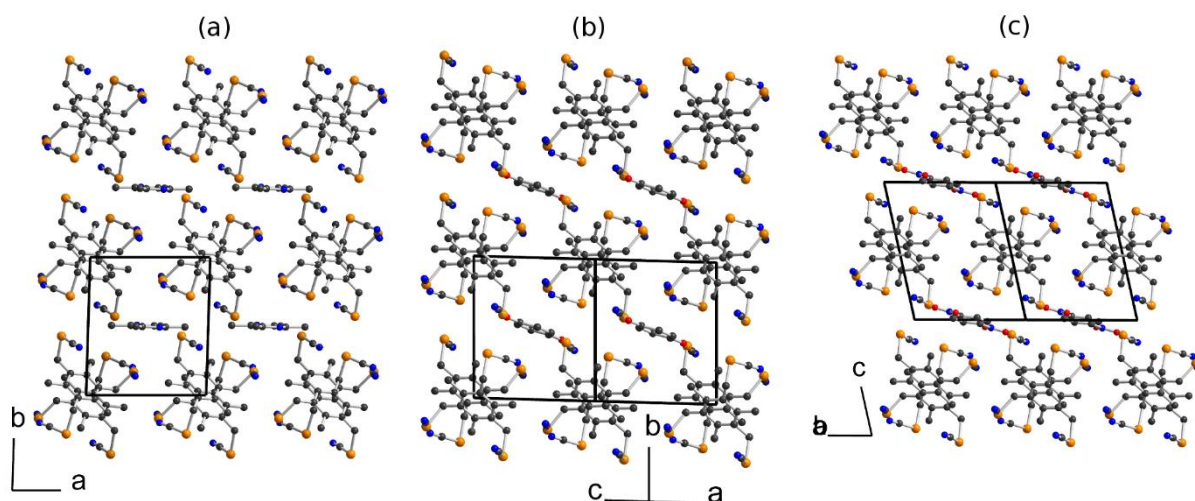


Figure 4. Solid state organization in (a) $(\mathbf{1})_2\cdot\text{TMP}$ viewed in projection along c axis, (b) $(\mathbf{1})_2\cdot\text{BQ}$ viewed in projection along $a+c$, and $(\mathbf{1})_2\cdot\text{pDNB}$ viewed in projection along $a-b$.

The efficiency of benzylic selenocyanates such as **1** to act as strong ChB donors can be traced back from the amplitude of the σ -hole generated on the selenium atom. As shown in Figure 5, the electrostatic surface potential (ESP) map calculated for **1** shows indeed the presence of positively charged areas in the prolongation of the three C–Se bonds, with $V_{s,\text{max}}$ of 41.1 kcal mol⁻¹. This value can be compared with that calculated for the model benzylselenocyanate PhCH₂–SeCN molecule where it amounts to 36.4 kcal mol⁻¹, or with that calculated for the reference halogen bond donor F₅C₆–I (35.7 kcal mol⁻¹) in the same conditions. These calculations demonstrate that tri-substitution actually activates the three individual ChB donor moieties.

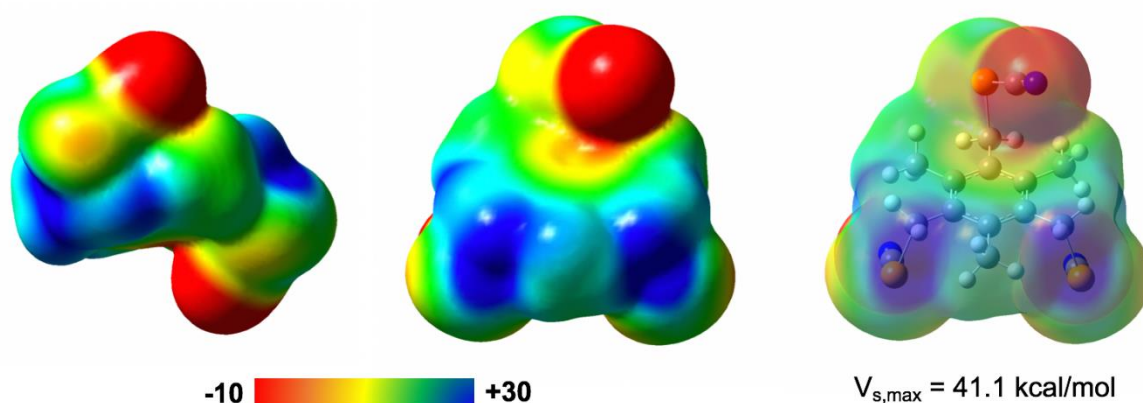


Figure 5. Three views of the computed electrostatic surface potential of **1** (0.001 a.u. molecular surface). Potential scale ranges from -10 kcal mol⁻¹ to 30 kcal mol⁻¹.

These similarities also demonstrate that the three ChB acceptors used here can play a very similar role as ditopic Lewis bases. An interesting analogy can be made with halogen bonding (XB) if we compare reported structures involving these three molecules (TMP, BQ, *p*DNB) and a common XB donor such as 1,4-diiodoperfluorobenzene. Indeed, *p*I₂F₄C₆ has been reported to co-crystallize with TMP (CCCD JAQMAQ; Syssa-Magale *et al.*, 2005) and BQ (CCDC ZARFUV; Liu *et al.*, 2012) while the non-fluorinated 1,4-diodobenzene has been co-crystallized with *p*DNB (CCDC YESZEB; Allen *et al.*, 1994). As shown in Figure 6, the three reported structures show a recurrent 1D structure where TMP, BQ and *p*DNB play also a similar role.

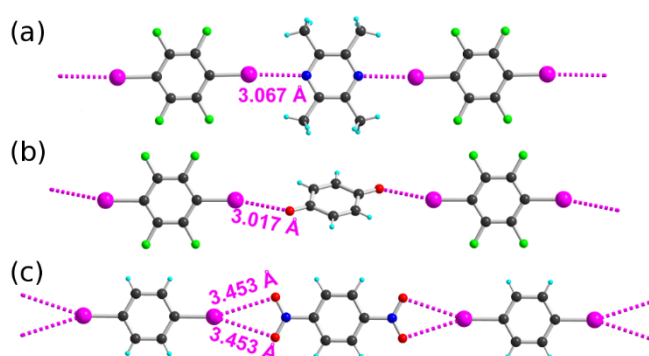


Figure 6. Detail of the one-dimensional structures stabilized by 1,4-diiodoperfluorobenzene XB with the three ditopic molecules (a) TMP, (b) BQ, and (c) *p*DNB, acting as analogous XB acceptors.

In conclusion, we have shown here that specific supramolecular motifs can be obtained from the ChB interaction of the *tris*-substituted derivative **1** with three different ditopic Lewis bases such as TMP, BQ or *p*DNB. The sizeable ChB interactions with the nitro group in DNB allow us to infer that benzylic selenocyanate derivatives such as **1** could be used for the detection of nitrated molecules of interest for their energetic properties, such as TNT (trinitrotoluene) or HNS (hexanitrostilbene), an issue of strong current interest (Schubert & Kuznetsov, 2012; Caygill *et al.*, 2012).

Experimental section

Crystal growth

Compound **1** was prepared as previously described (Jeannin *et al.*, 2018). All cocrystals were obtained from vapor diffusion of diethyl ether into ethyl acetate (2 mL) mixtures of two

equivalents of **1** (10.7 mg, 11 mg and 10.8 mg respectively) and one equivalent of either TMP (2.2 mg), BQ (3.5 mg) or *p*DNB (2.8 mg).

Crystallography. Single crystal X-ray diffraction data were collected at room temperature on an APEXII, Bruker-AXS diffractometer operating with graphite-monochromated Mo-K α radiation ($\lambda = 0.71073 \text{ \AA}$). The structures were solved by direct methods using the SIR92 program (Altomare *et al.*, 1994) and then refined with full-matrix least-square methods based on F2 (SHELXL-2014/7) (Sheldrick, 2015) with the aid of the WINGX program (Farrugia, 2012). All non-hydrogen atoms were refined with anisotropic atomic displacement parameters. H atoms were finally included in their calculated positions. Crystallographic data on X-ray data collection and structure refinements are given in Table 2.

Table 2. Crystallographic data

	TMP	BQ	<i>p</i> DNB
Formula	C ₁₉ H ₂₁ N ₄ Se ₃	C ₁₈ H ₁₇ N ₃ OSe ₃	C ₁₈ H ₁₇ N ₄ O ₂ Se ₃
Formula moiety	C ₁₅ H ₁₅ N ₃ Se ₃ , 0.5(C ₈ H ₁₂ N ₂)	C ₁₅ H ₁₅ N ₃ Se ₃ , 0.5(C ₆ H ₄ O ₂)	C ₁₅ H ₁₅ N ₃ Se ₃ , 0.5(C ₆ H ₄ N ₂ O ₄)
Crystal size	0.13×0.04×0.02	0.28×0.02×0.01	0.31×0.03×0.01
FW (g.mol ⁻¹)	542.28	528.23	558.23
System	triclinic	triclinic	triclinic
Space group	<i>P</i> $\bar{1}$	<i>P</i> $\bar{1}$	<i>P</i> $\bar{1}$
<i>a</i> (Å)	9.797(3)	10.008(2)	10.187(3)
<i>b</i> (Å)	10.560(3)	10.4345(19)	10.415(2)
<i>c</i> (Å)	10.656(3)	10.760(2)	11.232(3)
α (deg)	87.528(10)	93.538(5)	75.891(8)
β (deg)	69.844(8)	117.528(5)	82.213(9)
γ (deg)	87.528(9)	95.282(5)	61.753(8)
<i>V</i> (Å ³)	1033.5(5)	985.3(3)	1017.8(5)
<i>T</i> (K)	296(2)	296(2)	296(2)
<i>Z</i>	2	2	2
<i>D</i> _{calc} (g.cm ⁻³)	1.743	1.781	1.821
μ (mm ⁻¹)	5.349	5.61	5.441
Total refls	25685	24136	16919
θ_{max} (°)	27.443	27.492	27.509

Abs corr	multi-scan	multi-scan	multi-scan
T _{min} , T _{max}	0.774, 0.899	0.874, 0.945	0.822, 0.947
Uniq. refls	4706	4486	4665
R _{int}	0.0573	0.0878	0.0497
Uniq. refls (I > 2σ(I))	2995	2412	2903
R ₁	0.0407	0.0538	0.0419
wR ₂ (all data)	0.0923	0.1404	0.1061
GOF	1.002	1.003	0.973
Res. dens. (e Å ⁻³)	0.701, -0.525	0.817, -0.657	1.104, -0.474

ESP Computation Details. Calculations were carried out with Gaussian '09 software package on a Linux workstation. Geometries for tris(selenocyanatomethyl)-2,4,6-trimethylbenzene **1** (See Table 1 in ESI) were optimized by DFT (B3LYP) calculations with 6-31+G** basis set for all atoms except selenium, and the LANL2DZdp ECP basis set for selenium. The LANLL2DZdp basis set for iodine was downloaded from the Basis Set Exchange (<https://bse.pnl.gov/bse/portal>). Geometry optimization employed tight convergence criteria, and frequency calculations confirmed that the optimum structure had no imaginary vibrational frequencies.

References

- Alkorta, I., Elguero, J. & Del Bene, J. E. (2018) *ChemPhysChem* **19**, 156–1765.
- Allen, F. H., Goud, B. S., Hoy, V. J., Howard, J. A. K. & Desiraju, G. R. (1994) *Chem. Commun.* 2729–2730.
- Altomare, A., Cascarano, G., Giacovazzo, C., Guagliardi, A., Burla, M. C., Polidori, G. & Camalli, M. (1994) *J. Appl. Cryst.* **27**, 435–436.
- Bauzá, A. & Frontera, A. (2018) *Molecules* **23**, 699 (1-11)
- Benz, S., Macchione, M., Verolet, Q., Mareda, J., Sakai, N. & Matile, S. (2016) *J. Am. Chem. Soc.* **138**, 9093–9096.
- Benz, S., Poblador-Bahamonde, A. I., Low-Ders, N. & Matile, S. (2018) *Angew. Chem. Int. Ed.* **57**, 5408–55412.
- Bleholder, C, Werz, D. B., Koppel, H. & Gleiter, R. (2006) *J. Am. Chem. Soc.* **128**, 2666–2674.
- Brezgunova, M., Lieffrig, J., Aubert, E., Dahaoui, S., Fertey, P., Lebègue, S., Angyan, J., Fourmigué, M. & Espinosa, E. (2013) *Cryst. Growth Des.* **13**, 3283–3289.

- Cavallo, G., Metrangolo, P., Pilati, T., Resnati, G. & Terraneo, G. (2014) *Cryst. Growth Des.* **14**, 2697–2702.
- Cavallo, G., Metrangolo, P., Milani, R., Pilati, T., Priimagi, A., Resnati, G. & Terraneo, G. (2016) *Chem. Rev.* **116**, 2478–2601.
- Caygill, J. S., Davis F. & Higson, S. P. J. (2012) *Talanta* **88**, 14–29.
- Farrugia, L. J. (2012) *J. Appl. Cryst.*, **45**, 849–854.
- Gilday, L. C., Robinson, S. W., Barendt, T. A., Langton, M. J., Mullaney, B. R. & Beer, P. D. (2015) *Chem. Rev.* **2015**, **115**, 7118–7195.
- Huynh, H.-T., Jeannin, O. & Fourmigué, M. (2017) *Chem. Commun.* **53**, 8467–8469.
- Jeannin, O., Huynh, H.-T., Riel, A. M. S. & Fourmigué, M. (2018) *New J. Chem.* **42**, 10502–10509.
- Klapötke, T. M., Krumm, B., Gálvez-Ruiz, J. C., Nöth, H. & Schwab, I. (2004) *Eur. J. Inorg. Chem.* 4764–4769.
- Klapötke, T. M., Krumm, B. & Scherr, M. (2008) *Inorg. Chem.* **47**, 7025–7028.
- Liu, P., Ruan, C., Li, T. & Ji, B. (2012) *Acta Crystallogr. E* **68**, o1431.
- Maartmann-Moe, K., Sanderud, K. A. & Songstad, J. (1984) *Acta Chem. Scand. A*, **38**, 187–200.
- Pascoe, D. J., Ling, K. B. & Cockroft, S. L. (2017) *J. Am. Chem. Soc.*, **139**, 15160–15167.
- Politzer, P., Murray, J. S., Clark, T. & Resnati, G. (2017) *Phys. Chem. Chem. Phys.* **19**, 32166–32178.
- Sánchez-Sanz, G. & Trujillo, C. (2018) *J. Phys. Chem. A* **122**, 1369–1377.
- Schubert, H. & Kuznetsov, A. Eds (2012). *Detection of Bulk Explosives Advanced Techniques against Terrorism: NATO ARW Proceedings*, Springer.
- Sheldrick, G. M. (2015) *Acta Cryst. C*, **71**, 3–8.
- Syssa-Magale, J.-L., Boubekour, K., Palvadeau, P., Meerschaut, A. & Schöllhorn, B. (2005) *CrystEngComm* **7**, 302–308.
- Wang, W., Ji, B. & Zhang, Y. (2009) *J. Phys. Chem. A* **113**, 8132–8135.
- Wang, H., Liu, J. & Wang, W. (2018) *Phys. Chem. Chem. Phys.* **20**, 5227–5234.
- Wonner, P., Vogel, L., Kniep, F. & Huber, S.M. (2017) *Chem. Eur. J.* **23**, 16972–16975.